JCI insight

Identification of microRNA-181a-5p and microRNA-4454 as mediators of facet cartilage degeneration

Akihiro Nakamura, … , Igor Jurisica, Mohit Kapoor

JCI Insight. 2016;1(12):e86820. https://doi.org/10.1172/jci.insight.86820.

Research Article **Cell biology**

Osteoarthritis (OA) of spine (facet joints [FJs]) is one of the major causes of severe low back pain and disability worldwide. The degeneration of facet cartilage is a hallmark of FJ OA. However, endogenous mechanisms that initiate degeneration of facet cartilage are unknown, and there are no disease-modifying therapies to stop FJ OA. In this study, we have identified microRNAs (small noncoding RNAs) as mediators of FJ cartilage degeneration. We first established a cohort of patients with varying degrees of facet cartilage degeneration (control group: normal or mild facet cartilage degeneration; FJ OA group: moderate to severe facet cartilage degeneration) and then screened 2,100 miRNAs and identified 2 miRNAs (miR-181a-5p and miR-4454) that were significantly elevated in FJ OA cartilage compared with control facet cartilage. We further explored their role, function, and signaling mechanisms using computational, in vitro functional, and in vivo studies. We specifically indicate that miR-181a-5p and miR-4454 are involved in promoting inflammatory, catabolic, and cell death activity in FJ chondrocytes. This is the first report to our knowledge that identifies miR-181a-5p and miR-4454 as mediators of cartilage degeneration in FJs and potential therapeutic targets for stopping cartilage degeneration.

JCI insight

RESEARCH ARTICLE

Identification of microRNA-181a-5p and microRNA-4454 as mediators of facet cartilage degeneration

Akihiro Nakamura,[1,2] Y. Raja Rampersaud,[1,3] Anirudh Sharma,[1,2] Stephen J. Lewis,[1,3] Brian Wu,[1,2] Poulami Datta,[1,2] Kala Sundararajan,[1,2] Helal Endisha,[1,2] Evgeny Rossomacha,[1,2] Jason S. Rockel,[1,2] Igor Jurisica,[4] and Mohit Kapoor[1,2,5]

[1]Arthritis Program and [2]Division of Genetics and Development, Krembil Research Institute, University Health Network, Toronto, Ontario, Canada. [3]Spinal Program, Krembil Neuroscience Center, Toronto Western Hospital, University Health Network, University of Toronto, Toronto, Ontario, Canada. [4]Princess Margaret Cancer Centre, University Health Network and Departments of Medical Biophysics and Computer Science, University of Toronto, Ontario, Canada. [5]Department of Surgery and Department of Laboratory Medicine and Pathobiology, University of Toronto, Ontario, Canada.

Osteoarthritis (OA) of spine (facet joints [FJs]) is one of the major causes of severe low back pain and disability worldwide. The degeneration of facet cartilage is a hallmark of FJ OA. However, endogenous mechanisms that initiate degeneration of facet cartilage are unknown, and there are no disease-modifying therapies to stop FJ OA. In this study, we have identified microRNAs (small noncoding RNAs) as mediators of FJ cartilage degeneration. We first established a cohort of patients with varying degrees of facet cartilage degeneration (control group: normal or mild facet cartilage degeneration; FJ OA group: moderate to severe facet cartilage degeneration) and then screened 2,100 miRNAs and identified 2 miRNAs (miR-181a-5p and miR-4454) that were significantly elevated in FJ OA cartilage compared with control facet cartilage. We further explored their role, function, and signaling mechanisms using computational, in vitro functional, and in vivo studies. We specifically indicate that miR-181a-5p and miR-4454 are involved in promoting inflammatory, catabolic, and cell death activity in FJ chondrocytes. This is the first report to our knowledge that identifies miR-181a-5p and miR-4454 as mediators of cartilage degeneration in FJs and potential therapeutic targets for stopping cartilage degeneration.

Introduction

The degeneration of facet cartilage is a hallmark of facet joint osteoarthritis (FJ OA). Radiographically, FJ OA appears similar to OA in appendicular synovial joints; however, the specific mechanisms associated with facet cartilage degeneration during FJ OA are largely unknown. Due to the lack of biomarkers, it is impossible to identify patients exhibiting early stages of FJ OA, leading to severe cartilage degeneration and associated low back pain (1). Furthermore, due to a poor understanding of the underlying mechanisms associated with the degeneration of facet cartilage, no targeted therapies to treat FJ OA exist to date. In order to devise appropriate therapeutic strategies to stop, reduce, or delay facet cartilage degeneration, it is critical to first identify endogenous mechanisms contributing to facet cartilage degeneration.

MicroRNAs (miRNAs) are small noncoding RNAs that are expressed as primary stem loop precursors and undergo maturation by enzymatic processes (2–4). The mature forms are single-stranded noncoding RNA molecules, which are 20–23 nucleotides in length, that usually bind to the 3′ untranslated region of the target mRNAs, resulting in mRNA destabilization or inhibition of translation (5). It is estimated that miRNAs regulate over 60% of all coding genes and play pivotal roles in physiological processes, including cell proliferation, differentiation, genomic stability, metabolism, apoptosis, and aging (6–8).

The role of miRNAs in facet cartilage degeneration is largely unknown. However, recent studies performed in knee or hip OA do suggest a pathophysiological role for some miRNAs during OA pathogenesis (9). miR-140 is the one of most widely investigated miRNAs in knee OA research. Cartilage-specific expression of miR-140 has been reported in zebrafish (10) and in mice (11). miR-140 regulates cartilage development and homeostasis, and its loss contributes to the development of an age-related knee OA–like phenotype (12).

Conflict of interest: The authors (MK, AN, and YRR) have filed a US provisional patent (62/299,305): miRNAs Biomarkers for Facet Cartilage Degeneration.

Submitted: February 1, 2016
Accepted: June 30, 2016
Published: August 4, 2016

Reference information:
JCI Insight. 2016;1(12):e86820.
doi:10.1172/jci.insight.86820.

miR-146 is another miRNA that is highly expressed in low-grade OA cartilage and is induced by IL-1β stimulation; additionally, it mediates chondrocyte apoptosis (13, 14). In serum, Beyer et al. recently reported miRNA let-7e as a potential predictor for severe knee or hip OA (15).

In this study, we sought to identify the role of miRNAs in cartilage degeneration associated with FJ OA. In a stepwise manner, we first established and validated a patient cohort with varying degrees of facet cartilage degeneration that demonstrated substantially different expression levels of key inflammatory, catabolic, anabolic, and cell death markers in the facet cartilage. Using this cohort, we performed a comprehensive screening of 2,100 miRNAs in facet cartilage. Screening, followed by validation studies, identified two miRNAs, namely miR-181a-5p and miR-4454, that were substantially upregulated in moderate to severe FJ OA cartilage compared with control facet cartilage (normal or mild degeneration). Further, functional studies in FJ OA chondrocytes were then performed using miR-181a-5p or miR-4454 mimic or inhibitor. Mimic experiments revealed that both miRNAs are involved in promoting the expression of inflammatory, catabolic, and cell death markers. Furthermore, inhibition of these miRNAs resulted in reversal of this destructive phenotype in vitro. Using a combination of computational and functional approaches, we further identified specific genes and pathways associated with miR-181a-5p and miR-4454 signaling in facet cartilage. Finally, by injecting miR-181a-5p mimic into rat FJs, we showed that miR-181a-5p is able to degenerate facet cartilage in vivo by enhancing chondrocyte apoptosis and cartilage catabolic activity, thus exhibiting phenotypic features of FJ OA. This study is the first to our knowledge to perform comprehensive screening and identification of miR-181a-5p and miR-4454 as mediators of cartilage degeneration.

Results

Establishment of a patient cohort with varying degrees of facet cartilage degeneration. FJs were obtained from L3-S1 spinal levels of FJ OA patients undergoing lumbar surgery for neurogenic claudication (n = 34; age range: 42–81 years old, mean age ± SEM: 65.5 ± 1.6 years old) due to lumbar spinal stenosis (LSS) or radiculopathy (n = 21; age range: 24–53 years old, mean age ± SEM: 34.1 ± 1.4 years old) due to lumbar disc herniation (LDH).

At the surgical level, the degree of FJ and intervertebral disc degeneration was assessed using MRI, as described by Weishaupt et al. (16) and Pfirrmann et al. (17), respectively (Figure 1A and Table 1). The facets in all patients from the LDH group exhibited a degenerative grade of 0 (normal; 38.1%) or 1 (mild; 61.9%) and thus formed our control group. Whereas all patients with surgery for LSS exhibited significantly greater FJ OA ($P < 0.01$): 26.5% of patients had grade 2 (moderate) FJ OA and 73.5% had grade 3 (severe) FJ OA (Table 1). No statistical differences ($P = 0.78$) in the degree of intervertebral disc degeneration were observed between two groups.

Qualitative histological analysis further showed normal or mild facet cartilage degeneration, proteoglycan loss, and loss of cellularity in control facet cartilage, whereas moderate to severe facet cartilage degeneration was observed in FJ OA cartilage with profound loss of proteoglycan and chondrocytes. Osteoarthritis Research Society International (OARSI) scoring, measured on a scale from 0 to 6 (18), showed significantly increased ($P < 0.01$) cartilage degeneration in facet cartilage from the FJ OA group compared with the control group (Figure 1B). Taken together, clinical imaging and histological analysis clearly show an enhanced degree of facet cartilage degeneration in the FJ OA group compared with the control group.

Expression of catabolic, inflammatory, and cell death markers and type II collagen in FJ OA cartilage. After confirming that facet cartilage degeneration in FJ OA patients exhibited greater severity, as assessed by MRI and histopathology, we next determined the expression of cartilage matrix molecule (type II collagen) and key catabolic, inflammatory, and cell death markers implicated in cartilage degeneration during OA pathogenesis in FJ OA cartilage and control cartilage.

Real-time PCR (RT-PCR) analysis showed, that compared with control cartilage, FJ OA cartilage exhibited an increase in the expression of major cartilage catabolic factor matrix metalloproteinase-13 (*MMP13*) ($P < 0.01$), and proinflammatory cytokines, such as *TNFA* ($P < 0.05$), *IL6* ($P < 0.05$), and monocyte chemoattractant protein-1 (*MCP1*) ($P < 0.01$), and a decrease in the expression of type II collagen mRNA (*COL2A1*) ($P < 0.05$), whose protein product is a major contributor to the cartilage matrix (Figure 1C). Furthermore, increased chondrocyte cell death/apoptosis was observed in FJ OA cartilage compared with control cartilage, as assessed by TUNEL and poly (ADP-ribose) polymerase (PARP) p85 immunostaining (Figure 1D). These results show enhanced catabolic, inflammatory, and cell death activity in chondrocytes and decreased anabolic activity in FJ OA cartilage compared with the control cartilage.

Table 1. Baseline characteristics and MRI grading assessment in control and facet joint osteoarthritis groups

	Control (n = 21)	FJ OA (n = 34)	
Age range (years old)	24–53	42–81	
Age mean ± SEM	34.1 ± 1.4	65.5 ± 1.6	$P < 0.01$
Male	8 (38.1)	16 (47.1)	
Female	13 (61.9)	18 (52.9)	
Surgical side			
Left	13 (61.9)	13 (38.2)	
Right	8 (38.1)	21 (61.8)	
Surgical level			
L 3/4	0	7 (20.6)	
L 4/5	7 (33.3)	17 (50.0)	
L 5/S1	14 (66.7)	10 (29.4)	
FJ degeneration grading			
0	8 (38.1)	0	$P < 0.01$
1	13 (61.9)	0	
2	0	9 (26.5)	
3	0	25 (73.5)	
Disc degeneration grading			
I	0	0	$P = 0.78$
II	1 (4.8)	0	
III	7 (33.3)	11 (32.4)	
IV	9 (42.9)	15 (44.1)	
V	4 (19.0)	8 (23.5)	

No statistical differences in the severity of lumbar disc degeneration were observed in either group ($P = 0.78$). The 2-tailed Student's t test and the χ^2 test were used to analyze age difference and gradings of FJ OA/disc degeneration in control versus FJ OA groups, respectively. FJ OA, facet joint osteoarthritis.

miRNA screening phase — identification of a panel of miRNAs that are differentially expressed in FJ OA cartilage compared with control cartilage. We next comprehensively screened the expression of miRNA species in phenotypically distinct facet cartilage (Figure 2A). Out of 2,100 miRNAs screened using the miRNA array, we identified a panel of miRNAs that were differentially expressed in the FJ OA cartilage (n = 2; each sample consisted of pooled cartilage specimens from n = 3 patients of similar MRI grade; FJ OA sample 1: grade 2, FJ OA sample 2: grade 3) compared with control facet cartilage (n = 2) (grade: 0). Specifically, we identified 7 miRNAs that exhibited greater than 2-fold change (Figure 2B), whereas 22 miRNAs exhibited greater than 1.5-fold change in FJ OA cartilage compared with control cartilage (Supplemental Figure 1; supplemental material available online with this article; doi:10.1172/jci.insight.86820DS1). Microarray data is accessible at the NCBI's Gene Expression Omnibus (GEO) repository (http://www.ncbi.nlm.nih.gov/geo/query/acc.cgi?acc=GSE79258).

Validation phase — elevated expression of miR-181a-5p and miR-4454 in FJ OA cartilage. miRNAs exhibiting greater than a 2-fold change in their expression between FJ OA cartilage compared with control cartilage, including hsa-miR-372-5p, hsa-miR-3158-5p, hsa-miR-711, hsa-miR-4454, hsa-miR-4534, hsa-miR-181a-5p, and hsa-miR-4484, were further subjected to RT-PCR analysis in n = 34 FJ OA cartilage samples and n = 21 control cartilage samples. Results showed that, of 7 miRNAs tested, only miR-181a-5p and miR-4454 were significantly upregulated ($P < 0.01$) in FJ OA compared with control cartilage (Figure 2C), with no significant differences in the expression of other 5 miRNAs (Supplemental Table 1). Further, ordinal logistic regression analysis showed a significant positive correlation between the expressions of miR-181a-5p ($P = 0.0082$) or miR-4454 ($P = 0.0061$) and the severity of FJ OA based on MRI clinical grading score (Figure 2D) (correlation coefficients were 0.42 for miR-181a-5p expression and 0.46 for miR-4454 expression; Supplemental Table 2). For miR-181a-5p, a 1-unit increase in the expression was associated with a 3.2-fold increase in odds of a higher FJ OA grade. For miR-4454, a 1-unit increase in the expression was associated with a 2.0-fold increase in odds of a higher FJ OA grade.

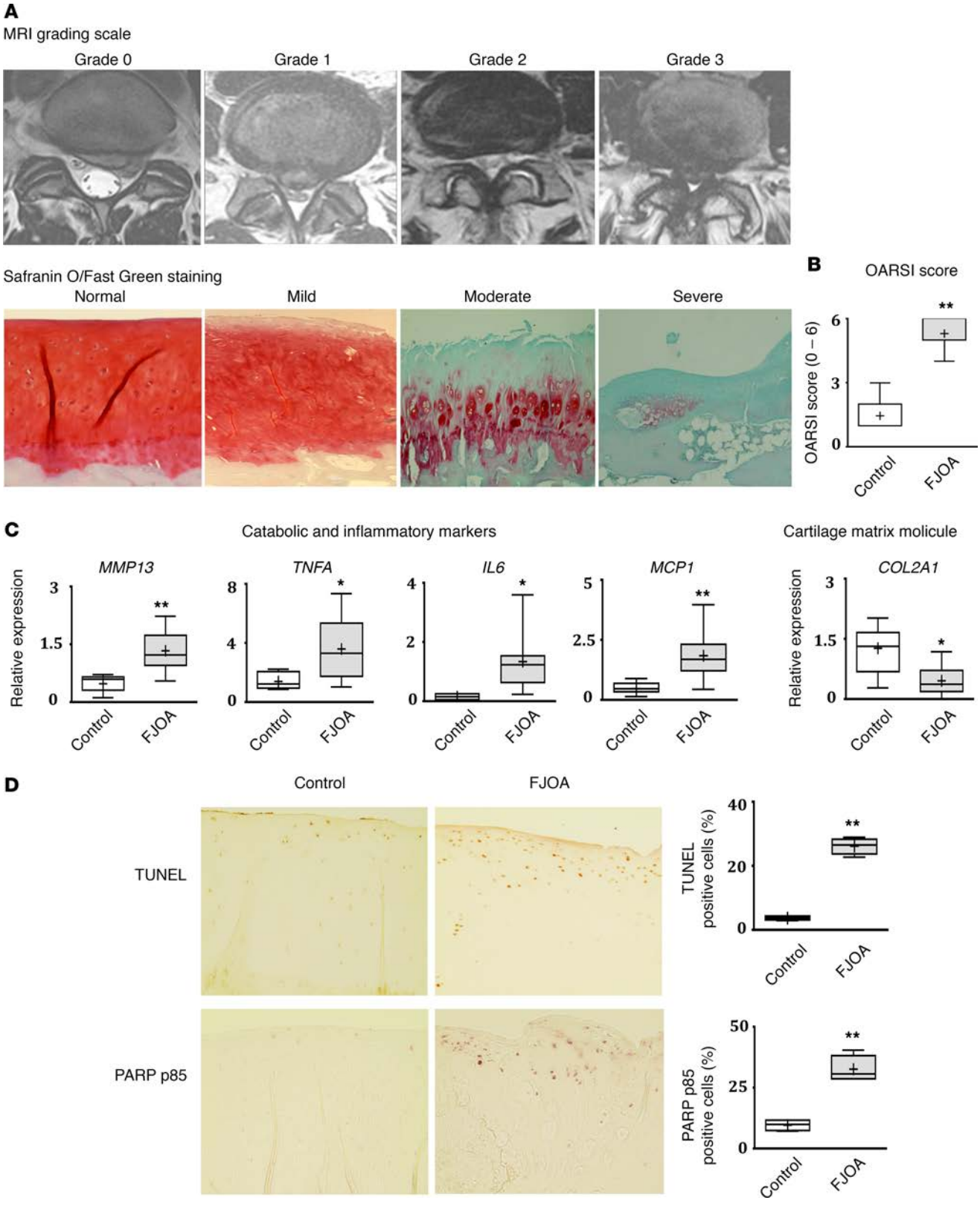
A
MRI grading scale
Grade 0
Grade 1
Grade 2
Grade 3
Safranin O/Fast Green staining
Normal
Mild
Moderate
Severe
B
OARSI score
OARSI score (0 – 6)
Control
FJOA
C
Catabolic and inflammatory markers
Cartilage matrix molicule
MMP13
TNFA
IL6
MCP1
COL2A1
Relative expression
D
Control
FJOA
TUNEL
PARP p85
TUNEL positive cells (%)
PARP p85 positive cells (%)

Figure 1. Establishment of a patient cohort with varying degrees of facet cartilage degeneration and MRI and histological analyses of facet joint degeneration. (**A**) Representative MRI of patients with lumbar disc herniation (LDH; *n* = 21) showing grade 0 (normal) or grade 1 (mild) facet joint (FJ) degeneration scores and FJ osteoarthritis (FJ OA; *n* = 34) patients showing grade 2 (moderate) or grade 3 (severe) FJ degeneration scores,exhibiting narrowed joint space and presence of osteophytes. Histological analysis using Safranin O/fast green staining showing facet cartilage with no degeneration, mild degeneration, moderate degeneration, and severe degeneration. Original magnification, ×10. (**B**) Osteoarthritis Research Society International (OARSI) scores in control (*n* = 21) and FJ OA (*n* = 34) cartilage. (**C**) Expression of OA catabolic, inflammatory, and matrix markers. Real-time PCR showed significant increases in the expression of major catabolic marker (*MMP13*) and inflammatory markers (*TNFA*, *IL6*, and *MCP1*) and a decrease in the expression of major cartilage matrix molecule (*COL2A1*) in FJ OA cartilage (*n* = 12) compared with control cartilage (*n* = 7). (**D**) Representative immunohistochemistry images of control (grade 0) and FJ OA cartilage (grade 3) stained for poly (ADP-ribose) polymerase (PARP) p85 and TUNEL. The number of PARP p85– and TUNEL-positive cells in FJ OA cartilage compared with control cartilage was quantified (*n* = 4/group). Original magnification, ×20. For data presented as box-and-whiskers plots, horizontal lines and cross marks indicate the medians and the means, boxes indicate 25th to 75th percentiles, and whiskers indicate minimum and maximum values of the data set. The significance of differences in the levels of expression between the control and FJ OA groups was determined using a 2-tailed Student's *t* test. $*P < 0.05$, $**P < 0.01$.

miR-181a-5p and miR-4454 mimics increase the expression of catabolic, inflammatory, and cell death markers and suppress type II collagen expression in FJ OA chondrocytes. After confirming the expression of miR-181a-5p and miR-4454 is markedly elevated in FJ OA cartilage compared with control cartilage, we further investigated if these miRNAs play a role in facet cartilage degeneration. Facet chondrocytes from FJ OA cartilage (*n* = 6/group) were treated with miR-181a-5p mimic or miR-4454 mimic or control mimic. We observed an increase in the mRNA expression of catabolic (*MMP13*) and inflammatory markers (*TNFA*, *IL6*, and *MCP1*) and protein expression of cell death marker (PARP p85) in facet chondrocytes treated with miR-181a-5p mimic (Figure 3, A and B). Facet chondrocytes treated with miR-4454 mimic also showed an increase in the expression of *TNFA*, *IL6*, *MCP1*, and PARP p85 but no significant increase in the expression of *MMP13*. Furthermore, we observed a decrease in the expression of *COL2A1* in FJ OA chondrocytes treated with either miR-181a-5p or miR-4454 mimic compared with the control mimic, suggesting that miR-181a-5p and miR-4454 promote catabolic, inflammatory, and cell death activity and suppress anabolic activity of FJ OA chondrocytes.

miR-181a-5p and miR-4454 inhibition suppress the expression of catabolic, inflammatory, and cell death markers and elevate type II collagen expression in IL-1β–treated FJ OA chondrocytes. Since miR-181a-5p and miR-4454 mimics increased expression of catabolic, inflammatory, and cell death markers and reduced the expression of *COL2A1*, we further tested if inhibition of these miRNAs can reverse these effects. As IL-1β is the major inflammatory/catabolic cytokine implicated in OA (19), FJ OA chondrocytes were treated with or without recombinant human IL-1β in the presence of miR-181a-5p, miR-4454, or control inhibitor. The expression of both miR-181a-5p and miR-4454 was markedly enhanced in response to IL-1β treatment (Figure 3C). Furthermore, IL-1β treatment increased the expression of *MMP13* and reduced the expression of *COL2A1* (Figure 3D). Treatment with either miR-181a-5p or miR-4454 inhibitor substantially suppressed *MMP13* and rescued the expression of *COL2A1* in IL-1β–treated cells. These results show that inhibition of miR-181a-5p or miR-4454 in IL-1β–treated FJ OA chondrocytes leads to a decrease in catabolic activity and increased anabolic activity.

We then assessed whether miR-181a-5p and miR-4454 inhibition could suppress the expression of inflammatory mediators in IL-1β–stimulated FJ OA chondrocytes. IL-1β treatment elevated the expression of *IL6*, *TNFA*, and *MCP1* in FJ OA chondrocytes. Inhibition of either miR-181a-5p or miR-4454 suppressed the expression of *IL6* (Figure 3D). However, the expression of *TNFA* and *MCP1* was substantially suppressed only by the miR-4454 inhibitor and not by the miR-181a-5p inhibitor. These results show that inhibition of miR-181a-5p or miR-4454 results in differential suppression of inflammatory mediators.

We further determined the effect of miR-181a-5p and miR-4454 inhibition on the level of PARP p85 in IL-1β–stimulated FJ OA chondrocytes. IL-1β treatment–mediated increases in the protein levels of PARP p85 were inhibited by both miR-181a-5p and miR-4454 inhibitors (Figure 3E). We have summarized the specific effects of the miR-181a-5p and miR-4454 mimics and inhibitors on the expression of inflammatory, catabolic, cell death, and cartilage matrix markers in Supplemental Table 3.

Signaling pathways modulated by miR-181a-5p and miR-4454. The potential gene targets and signaling pathways for miR-181a-5p and miR-4454 in the facet cartilage have never been reported; we therefore applied an integrative, computational biology approach to predict gene targets and signaling pathways regulated by both miR-181a-5p and miR-4454. Potential target genes for miR-181a-5p and miR-4454 were identified using mirDIP, focusing only on the middle third, top third, and top 1% of targets (Figure 4A). Taking the most likely targets of miR-181a-5p and miR-4454, we then identified the most frequently

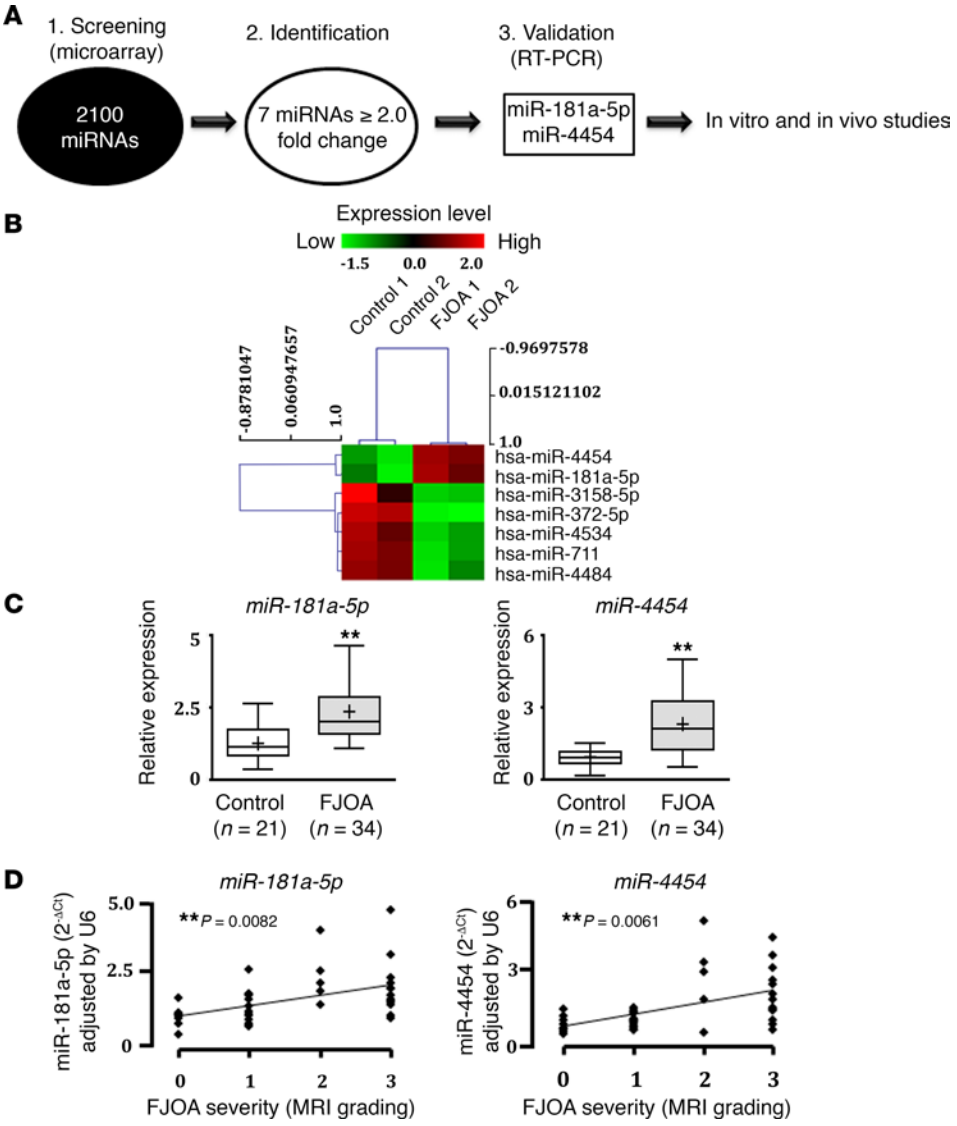

Figure 2. Screening, identification, and validation of microRNAs. (**A**) Schematic of study design. (**B**) Heatmap of differentially expressed microRNAs (miRNAs) (≥2.0-fold change) in facet joint osteoarthritis (FJ OA) cartilage (n = 2 MRI grade 2 and 3; each sample constitutes pooled cartilage specimens from 3 patients of similar MRI grade) and control cartilage (n = 2; grade 0). (**C**) Significant increase in the expression of miR-181a-5p and miR-4454 in FJ OA cartilage (n = 34) compared with control cartilage (n = 21), as assessed by real-time PCR. Data are presented as box-and-whiskers plots. Horizontal lines and cross marks indicate the medians and the means, boxes indicate 25th to 75th percentiles, and whiskers indicate minimum and maximum values of the data set. The significance of differences in the levels of expression between the control and FJ OA groups was determined using a 2-tailed Student's t test. $^{**}P < 0.01$. (**D**) Correlation between the expression of miR-181a-5p or miR-4454 and the severity of FJ OA based on MRI grading. Ordinal logistic regression model showing a significant positive correlation between the expression of miR-181a-5p (P = 0.0082) or miR-4454 (P = 0.0061) and MRI grading score (total = 55 patients: 21 from the control group and 34 from the FJ OA group). $^{**}P <$ 0.01. The significance of the correlation between miRNA expression and FJ OA grade was determined by 2-tailed t-test of the miRNA coefficient in each ordinal regression model.

enriched pathways using pathDIP. While 247 pathways were enriched (Supplemental Table 4), we identified the most frequent pathways associated with both miR-181a-5p and miR-4454. Specifically, the top 1% of individual target genes were related to the NF-κB signaling pathway.

To test these predictions, we treated FJ OA chondrocytes with miR-181a-5p mimic, miR-4454 mimic, or control mimic and determined the expression of the 10 predicted genes (zinc finger protein 454 [*ZNF454*], zinc finger protein 440 [*ZNF440*], mixed-lineage leukemia 1 [*MLL1*], lysine demethylase 5A [*KDM5A*], eukaryotic translation initiation factor 4A2 [*EIF4A2*], membrane bound O-acyltransferase domain containing 2 [*MBOAT2*], ATM serine/threonine kinase [*ATM*], leucine rich repeat containing 32 [*LRRC32*], la ribonucleoprotein domain family member 4 [*LARP4*], and caspase recruitment domain family member 8 [*CARD8*]) regulated by both miR-181a-5p and miR-4454. Results showed that, of all 10 genes tested, 8 genes did not exhibit any marked differences in their expression in response to miR-181a-5p or miR-4454 mimic in FJ OA chondrocytes. Interestingly, expression of *ZNF440* was substantially increased by both miR-181a-5p mimic and miR-4454 mimic compared with control mimic (Figure 4B). The expression of *MBOAT2* was only elevated in response to miR-181a-5p mimic (Supplemental Table 5).

To further test the involvement of ZNF440 in miR-181a-5p and miR-4454 signaling, we next treated FJ OA chondrocytes with IL-1β in the presence or absence of miR-181a-5p or miR-4454 inhibitor. IL-1β increased the expression of *ZNF440*, and this expression was suppressed by both miR-181a-5p and miR-4454 inhibitors (Figure 4C), suggesting that ZNF440 may play a role in miR-181a-5p and miR-4454 signaling in facet chondrocytes.

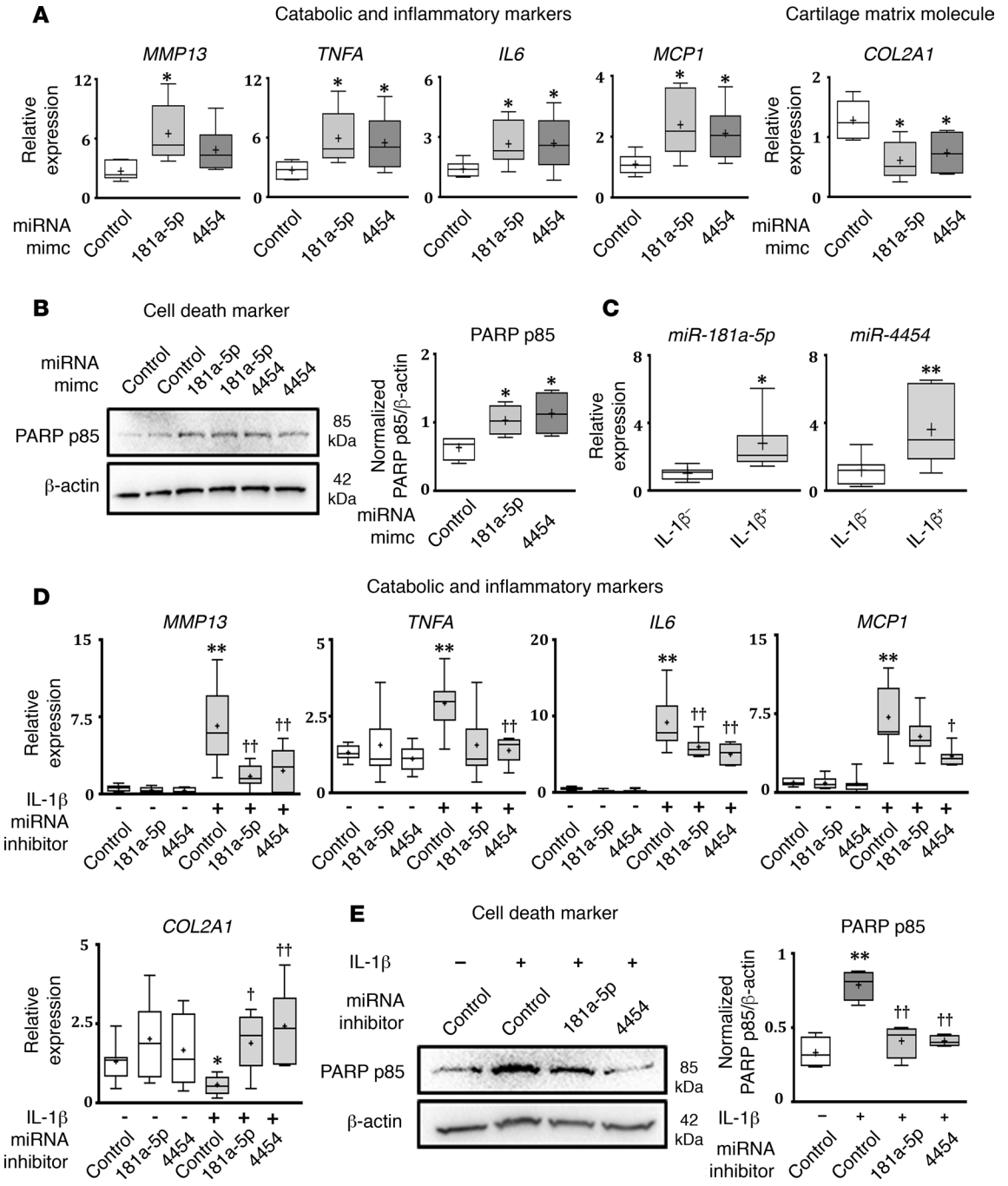

Figure 3. Effect of miR-181a-5p and miR-4454 mimics or inhibitors on the expression of catabolic, inflammatory, cell death, and matrix markers in facet joint osteoarthritis chondrocytes. (**A**) Real-time PCR (RT-PCR) analysis of the expression of major cartilage catabolic (*MMP13*) and inflammatory (*TNFA*, *IL6*, and *MCP1*) markers and the cartilage matrix molecule *COL2A1* in facet joint osteoarthritis (FJ OA) chondrocytes treated with miR-181a-5p or miR-4454 mimic compared with control mimic (n = 6/treatment). (**B**) PARP p85 expression relative to β-actin expression by Western blotting in FJ OA chondrocytes treated with miR-181a-5p or miR-4454 mimic compared with control mimic. Representative blot from n = 4 separate blots. Full uncut blots are shown in the supplemental figure. (**A** and **B**) *P < 0.05 between control and miR-181a-5p or miR-4454 mimics, as determined by 2-tailed Student's t test. (**C**) RT-PCR analysis of miR-181a-5p and miR-4454 in FJ OA chondrocytes treated with (+) or without (–) IL-1β (n = 7/treatment). *P < 0.05, **P < 0.01, as determined by a 2-tailed Student's t test. (**D**) RT-PCR analysis of catabolic, inflammatory, and cell death markers and *COL2A1* in FJ chondrocytes treated with or without IL-1β and miR-181a-5p, miR-4454, or control inhibitors (n = 7/treatment). (**E**) Immunoblot analysis of PARP p85 protein levels relative to β-actin in FJ OA chondrocytes treated with miR-181a-5p and miR-4454 inhibitors compared with control inhibitor in the presence or absence of IL-1β. Representative blot from n = 4 separate blots. Full uncut blots are shown in the supplemental figure. (**D** and **E**) Differences in the levels of expression among miR-181a-5p, miR-4454, and control inhibitors with or without IL-1β treatment were determined 1-way analysis of variance followed by Tukey's post-hoc tests.*P < 0.05, **P < 0.01, control inhibitor without IL-1β treatment vs. control inhibitor with IL-1β treatment. †P < 0.05, ††P < 0.01, control inhibitor treatment vs. miR-181a-5p or miR-4454 inhibitor treatment in the presence of IL-1β, respectively. All other comparisons were not significantly different (P > 0.05). For data presented as box-and-whiskers plots, horizontal lines and cross marks indicate the medians and the means, boxes indicate 25th to 75th percentiles, and whiskers indicate minimum and maximum values of the data set.

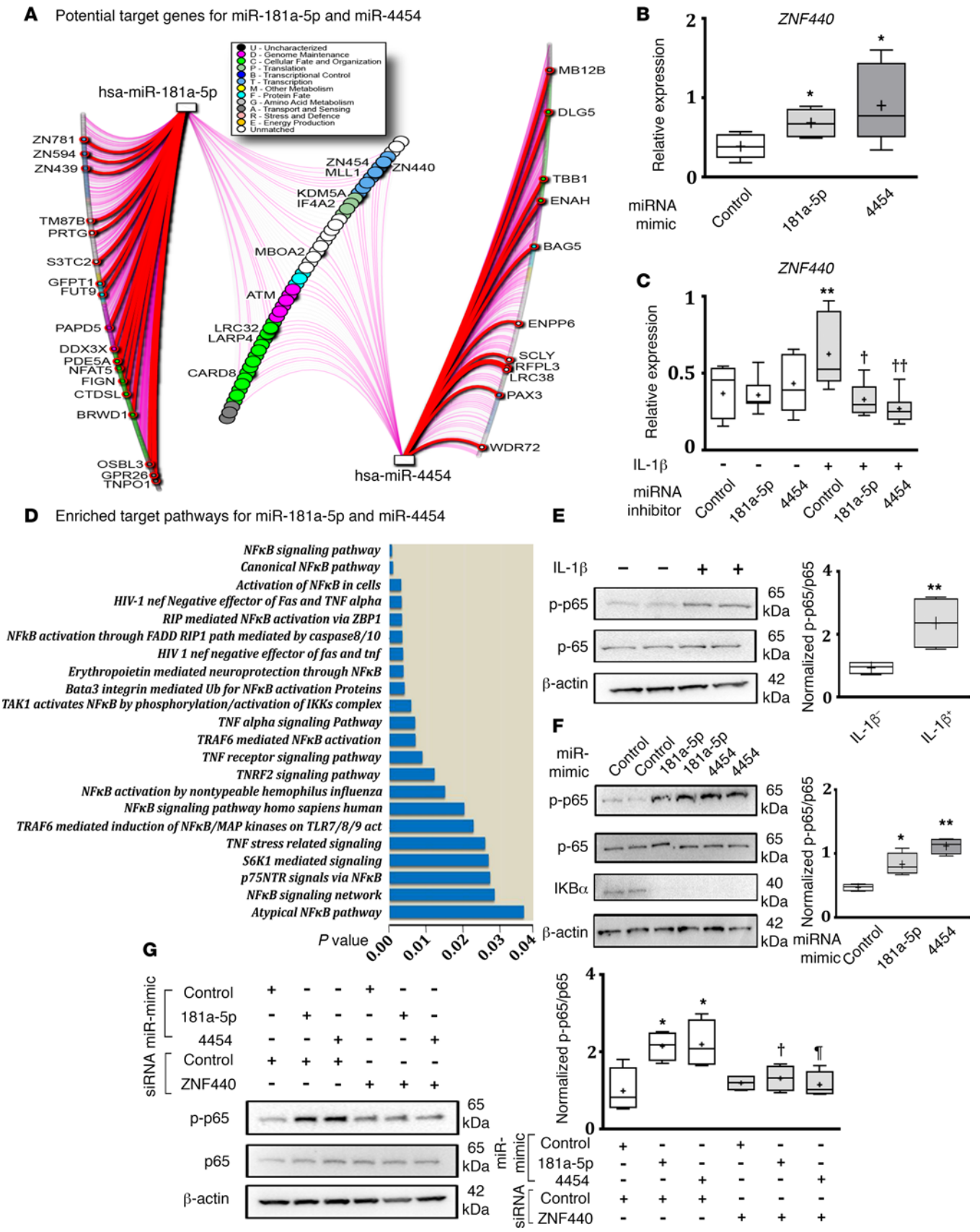
A
Potential target genes for miR-181a-5p and miR-4454
U - Uncharacterized
D - Genome Maintenance
C - Cellular Fate and Organization
P - Translation
B - Transcriptional Control
T - Transcription
M - Other Metabolism
F - Protein Fate
G - Amino Acid Metabolism
A - Transport and Sensing
R - Stress and Defence
E - Energy Production
Unmatched
hsa-miR-181a-5p
ZN781
ZN594
ZN439
TM87B
PRTG
S3TC2
GFPT1
FUT9
PAPD5
DDX3X
PDE5A
NFAT5
FIGN
CTDSL
BRWD1
OSBL3
GPR26
TNPO1
ZN454
MLL1
ZN440
KDM5A
IF4A2
MBOA2
ATM
LRC32
LARP4
CARD8
MB12B
DLG5
TBB1
ENAH
BAG5
ENPP6
SCLY
RFPL3
LRC38
PAX3
WDR72
hsa-miR-4454
B
ZNF440
Relative expression
miRNA mimic
Control
181a-5p
4454
C
ZNF440
Relative expression
IL-1β
miRNA inhibitor
Control
181a-5p
4454
D
Enriched target pathways for miR-181a-5p and miR-4454
NFκB signaling pathway
Canonical NFκB pathway
Activation of NFκB in cells
HIV-1 nef Negative effector of Fas and TNF alpha
RIP mediated NFκB activation via ZBP1
NFkB activation through FADD RIP1 path mediated by caspase8/10
HIV 1 nef negative effector of fas and tnf
Erythropoietin mediated neuroprotection through NFκB
Bata3 integrin mediated Ub for NFκB activation Proteins
TAK1 activates NFκB by phosphorylation/activation of IKKs complex
TNF alpha signaling Pathway
TRAF6 mediated NFκB activation
TNF receptor signaling pathway
TNRF2 signaling pathway
NFκB activation by nontypeable hemophilus influenza
NFκB signaling pathway homo sapiens human
TRAF6 mediated induction of NFκB/MAP kinases on TLR7/8/9 act
TNF stress related signaling
S6K1 mediated signaling
p75NTR signals via NFκB
NFκB signaling network
Atypical NFκB pathway
P value
E
IL-1β
p-p65
p-65
β-actin
65 kDa
42 kDa
Normalized p-p65/p65
IL-1β-
IL-1β+
F
miR-mimic
Control
181a-5p
4454
IKBα
40 kDa
miRNA mimic
G
siRNA miR-mimic
Control
181a-5p
4454
siRNA
ZNF440
p-p65
p65
β-actin
miR-mimic

Figure 4. microRNA-181-a-5p and -4454 target genes. (**A**) Potential target genes for miR-181a-5p and miR-4454 were identified using mirDIP version 2, focusing only on middle third, top third, and top 1% of targets. The microRNA (miRNA) gene network was visualized using NAViGaTOR version 2.3 and highlights shared targets (central nodes in the network) and individual target predictions (left and right lists). Thick red edge signifies the top 1% of prediction (corresponding genes are highlighted with red and named); purple edge signifies top-third predictions; all other edges correspond to middle third predictions. Shared targets predicted with top-third hits are highlighted. (**B**) RT-PCR analysis of zinc finger 440 (*ZNF440*) expression in facet joint osteoarthritis (FJ OA) chondrocytes treated with miR-181a-5p or miR-4454 mimic compared with control mimic (n = 6/treatment). *P < 0.05, comparing control mimic vs. miR-181a-5p or miR-4454 mimic, as determined by 2-tailed Student's t tests. (**C**) RT-PCR analysis *ZNF440* expression of FJ chondrocytes treated with (+) or without (–) IL-1β and miR-181a-5p, miR-4454, or control inhibitors (n = 7/treatment). **P < 0.01, control inhibitor with IL-1β vs. control inhibitor without IL-1β treatment; †P < 0.05, ††P < 0.01, control inhibitor vs. miR-181a-5p or miR-4454 inhibitor in the presence of IL-1β, as determined by 1-way analysis of variance followed by Tukey's post-hoc tests. (**D**) The most significantly enriched pathways for miR-181a-5p and miR-4454 targets using randomization test include NF-κB pathways, as identified by pathDIP version 1.0. (**E**) Immunoblot analysis of phosphorylation of Ser536 on NF-κB-p65 (p-p65) in FJ chondrocytes treated with or without IL-1β. (**F**) Immunoblot analysis of p-p65 and IκBα in FJ chondrocytes treated with miR-181a-5p, miR-4454, or control mimics. (**E** and **F**) Representative blots from n = 4 separate blots. Full uncut blots are shown in the supplemental figure. *P < 0.05, **P < 0.01, compared with untreated or control mimic, as determined by 2-tailed Student's t test. (**G**) Immunoblot analysis of p-p65 in response to miR-181a-5p mimic or miR-4454 mimic and/or ZNF440 siRNA. Representative blot from n = 4 separate blots. Full uncut blots are shown in the supplemental figure. *P < 0.05, control mimic/control siRNA vs. miR-181a-5p mimic/control siRNA or miR-4454 mimic/control siRNA, †P < 0.05, miR-181a-5p mimic/control siRNA vs. miR-181a-5p/ZNF440 siRNA treatment. ¶P < 0.05, miR-4454 mimic/control siRNA vs. miR-4454 mimic/ZNF siRNA treatment, as determined by 1-way analysis of variance followed by Tukey's post-hoc tests. For data presented as box-and-whiskers plots, horizontal lines and cross marks indicate the medians and the means, boxes indicate 25th to 75th percentiles, and whiskers indicate minimum and maximum values of the data set. See also Supplemental Figure 2 and Supplemental Table 4 and 5.

Based on our prediction data, the NF-κB signaling pathway showed significant association with both miR-181a-5p and miR-4454 (Figure 4D). NF-κB is negatively regulated by IκB, which retains NF-κB in the cytoplasm and thereby inhibits NF-κB –meditated transcription (canonical, IκB-dependent regulation; ref. 20), whereas phosphorylation of NF-κB p-65 on Ser536 renders NF-κB p-65 active irrespective of IκB expression (IκB-independent regulation; ref. 21). We first determined the phosphorylation of Ser536 of the NF-κB p-65 subunit, a marker of IκB-independent activity, in FJ OA chondrocytes treated with IL-1β. IL-1β treatment resulted in increased phosphorylation of Ser536 NF-κB p65 in FJ OA chondrocytes (Figure 4E). Furthermore, treatment with miR-181a-5p or miR-4454 mimic alone enhanced the phosphorylation of Ser536 NF-κB p65. Interestingly, miR-181a-5p or miR-4454 mimic also decreased the expression of IκBα in chondrocytes (Figure 4F), suggesting that NF-κB activity can be modulated by miR-181a-5p or miR-4454 by regulating both IκB-dependent and –independent NF-κB regulatory pathways. To further explore the role of ZNF440 on IκB-independent NF-κB p-65 activation in response to miR-181a-5p and miR-4454 signaling, we cotransfected FJ OA chondrocytes with either miR-181a-5p or miR-4454 mimic in the absence or presence of ZNF440 siRNA to determine the effect of silencing ZNF440 on the phosphorylation of Ser536 of NF-κB p65. Cotransfection of chondrocytes with ZNF440 siRNA resulted in a substantial knockdown in the expression of *ZNF440* (Supplemental Figure 2). Further, as expected, Western blot analysis showed an increased phosphorylation of Ser536 NF-κB p65 in response to miR-181a-5p or miR4454 mimic in the presence of control siRNA; however, these increases in phosphorylation of Ser536 NF-κB p65 were attenuated by ZNF440 siRNA (Figure 4G), suggesting a crucial role of ZNF440 in regulating IκB-independent NF-κB signaling downstream of miR-181a-5p and miR-4454 in FJ OA chondrocytes.

miR-181a-5p mimic promotes facet cartilage degeneration in vivo. Our in vitro studies using FJ OA chondrocytes treated with miR-181a-5p or miR-4454 mimic or inhibitor suggest that these miRNAs may play a role in facet cartilage degeneration by promoting catabolic, inflammatory, and cell death mechanisms. The next logical step was to test if these miRNAs initiate cartilage destructive activity in vivo. We used miR-181a-5p mimic for our animal studies. We injected miR-181a-5p mimic (right side) or control mimic (left side) into FJs (L4/5 and L5/6) of rats through the joint capsule (Figure 5A). Rats that underwent only surgical procedure without injection composed the sham group (Figure 5B). At 3 weeks after injections, FJs were extracted and subjected to histopathology and immunohistochemistry. Histopathological analysis of Safranin O/Fast green–stained FJ cartilage sections in combination with OARSI scoring showed that miR-181a-5p mimic treatment resulted in a FJ OA–like phenotype, with marked degeneration of facet cartilage associated with loss of chondrocyte cellularity and proteoglycan depletion compared with control mimic injection (Figure 5, C–I). Immunohistochemical analysis using PARP p85 antibody as a marker of chondrocyte apoptosis further showed a substantial increase in PARP p85–positive cells in miR-181a-5p mimic–treated FJs compared with control mimic–treated FJs (Figure 5, J–L, and P). Furthermore, immunohistochemical analysis using MMP13 antibody to account for cartilage catabolic activity showed markedly increased numbers of

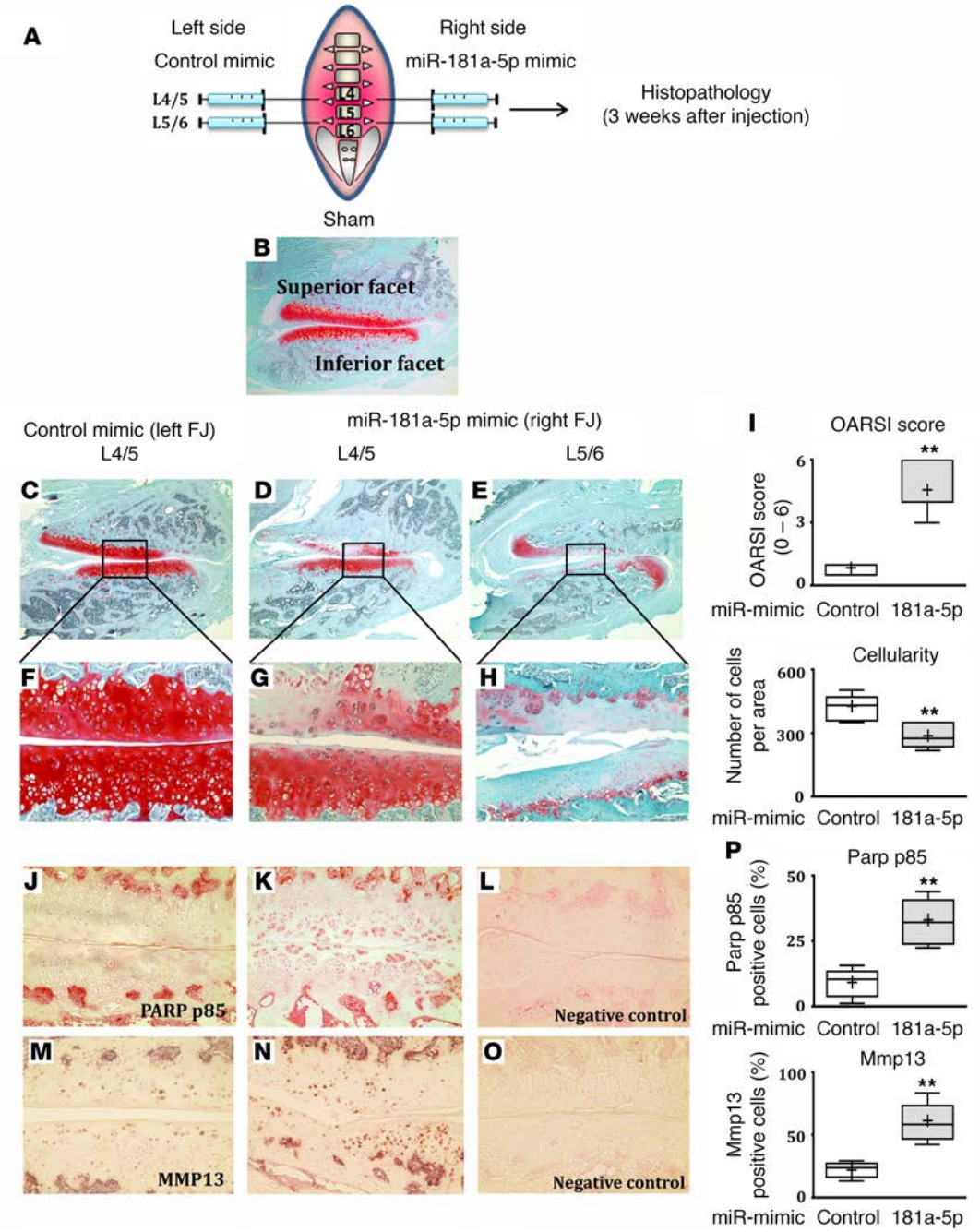

Figure 5. miR-181a-5p mimic promotes cartilage degeneration in vivo. (**A**) Schematic of miR-181a-5p mimic injection in facet joints (FJs) of rats of miR-181a-5p mimic (right side; $n = 7$) or control mimic (left side; $n = 7$ were injected into 2 lumbar spinal FJs, L4/5 and L5/6), using a 26-gauge Hamilton syringe under surgical microscope. (**B–H**) Rat FJs (L4/5 and L5/6) were stained with Safranin O/fast green stain. miR-181a-5p mimic injection resulted in a FJ OA–like phenotype associated with loss of chondrocyte cellularity, proteoglycan depletion, and cartilage degeneration in vivo. (**B**) Sham – without injection. (**C** and **F**) L4/5 FJ treated with control mimic. (**D** and **G**) L4/5 FJ treated with miR-181a-5p mimic. (**E** and **H**) L5/6 FJ treated with miR-181a-5p mimic. (**B–E**: original magnification, ×4; **F–H**: original magnification, ×20). (**I**) Histomorphometric analysis of FJs treated with miR-181a-5p or control mimic was scored by Osteoarthritis Research Society International (OARSI) scoring. Facet chondrocyte cellularity per area was calculated in FJs treated with miR-181a-5p or control mimic ($n = 7$/each group). (**J–P**) Representative images of FJ cartilage sections analyzed by immunohistochemistry for poly (ADP-ribose) polymerase (PARP) p85 or matrix metallopeptidase 13 (MMP13) ($n = 7$/each group). (**P**) Immuno-positive cells and total cells in FJ cartilage were counted and expressed as a percentage of PARP p85– and MMP13-positive cells. (**L** and **O**) Rabbit IgG-HRP was used as an isotype negative control (original magnification, ×20). (**I** and **P**) For data presented as box-and-whiskers plots, horizontal lines and cross marks indicate the medians and the means, boxes indicate 25th to 75th percentiles, and whiskers indicate minimum and maximum values of the data set. $^{**}P < 0.01$, as determined by 2-tailed Student's t tests.

MMP13-expressing cells in miR-181a-5p mimic–treated FJs compared with control mimic–treated FJs (Figure 5, M–P). These findings show that miR-181a-5p promotes facet cartilage degeneration, chondrocyte death, and catabolic activity in vivo.

Discussion

The endogenous mechanisms associated with the degeneration of facet cartilage during FJ OA are largely unknown. One of the biggest hurdles in FJ OA research has been the inability to adequately identify patients with varying degrees of facet cartilage degeneration and severity. Such identification and characterization is critical for studying the true mechanisms of cartilage degeneration. To understand the endogenous mechanisms associated with facet cartilage degeneration, we first created a unique biobank of facet cartilage with varying degrees of degeneration. We sequentially assessed the degree of FJ degeneration in two clinically distinct cohorts of patients undergoing lumbar spinal surgery. MRI analysis showed that all LSS patients exhibited substantially greater FJ degeneration compared with all LDH patients. The distinct degree of FJ degeneration between the patient groups was further assessed by histological analysis using OARSI scoring. Molecular assessment of FJ cartilage revealed enhanced expression of inflammatory, catabolic, and cell death markers as well as reduced expression of the major cartilage matrix molecule (*COL2A1*) in FJ OA compared with control facet cartilage. To our knowledge, this is the most validated cohort of patients exhibiting varying degrees of facet cartilage degeneration.

Our comprehensive characterization of lumbar facet cartilage enabled the evaluation of miRNA expression in facet cartilage at different stages of degeneration. We identified a panel of miRNAs (out of 2,100 miRNAs screened by array analysis) that exhibited differential expression in FJ OA compared with control cartilage. With further validation using RT-PCR analysis of a panel of 7 miRNAs (with greater than 2-fold change in FJ OA cartilage compared with control cartilage), we identified two specific miRNAs (miR-181a-5p and miR-4454) that were markedly elevated in the FJ OA cartilage compared with control cartilage, with no significant difference in the expression of other miRNAs. Remarkably, the expression of both miR-181a-5p and miR-4454 exhibited significant, positive correlations with the severity of FJ OA based on MRI grading.

To date, no study has reported the identification of miR-181a-5p and miR-4454 in facet cartilage or upregulation in FJ OA. However, recent studies performed in chondrocytes isolated from chicken sternal cartilage show that miR-181a reduces the expression of *COL2A1* (22). Gabler et al. showed that the expression of miR-181a is increased during hypertrophic chondrocyte differentiation in human mesenchymal stromal cells treated with transforming growth factor-β (23). Song et al. also reported that miR-181b, a member of the miR-181 family, was upregulated in OA chondrocytes isolated from patients with knee OA (24).

To determine if miR-181a-5p and miR-4454 play a pathophysiological role in facet cartilage degeneration, we extracted facet chondrocytes from FJ OA patients and treated these chondrocytes with miR-181a-5p or miR-4454 mimic to determine the effect on the expression of major OA catabolic, inflammatory, and cell death mediators as well as the anabolic cartilage matrix molecule, type II collagen. Our results showed that miR-181a-5p mimic and miR-4454 mimic were able to elevate the expression of inflammatory, catabolic, and cell death markers and decrease the expression of *COL2A1* compared with control mimic, suggesting that these miRNAs promote destructive mechanisms in FJ chondrocytes. Using miR-181a-5p and miR-4454 inhibitors in FJ OA chondrocytes stimulated with IL-1β, we showed that inhibition of miR-181a-5p or miR-4454 suppressed the expression of inflammatory, catabolic and cell death markers and elevated the expression of *COL2A1* in FJ OA chondrocytes. Consistent with our results, attenuation of miR-181b, using miR-181b inhibitor, reduced *MMP13* expression and increased *COL2A1* expression in chondrocytes. Interestingly, overexpression of anti–miR-181b significantly reduced cartilage destruction in a mouse model of knee OA (24). These results suggest a role for miR-181a-5p and miR-4454 as mediators of cartilage degeneration.

Since signaling mechanisms through which miR-181a-5p and miR-4454 operate in the facet cartilage have not been reported, we applied a computational biology approach and identified 10 potential genes commonly regulated by both miR-181a-5p and miR-4454. Validation studies of all 10 predicted genes indicated that only *ZNF440* was substantially elevated by both miR-181a-5p mimic and miR-4454 mimic in FJ OA chondrocytes. Furthermore, IL-1β–mediated elevation in the expression of *ZNF440* was suppressed in the presence of miR-181a-5p or miR-4454 inhibitors, suggesting a crucial role of *ZNF440* in miR-181a-5p or miR-4454 signaling in FJ OA chondrocytes. IL-1β has been previously shown to activate NF-κB in human

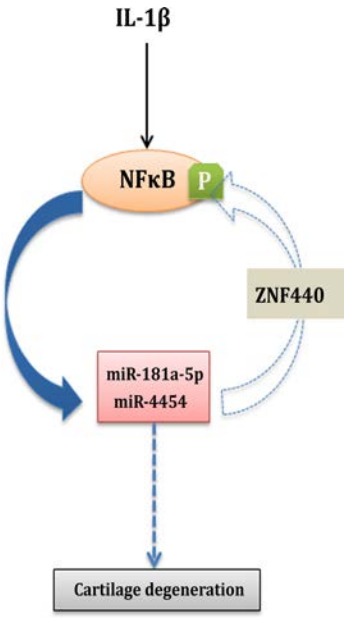

Figure 6. Schematic of miR-181a-5p and miR-4454 signaling in facet joint chondrocytes. IL-1β–mediated activation of NF-κB signaling may upregulate miR-181a-5p and miR-4454 expression, resulting in a positive feedback loop to sustain NF-κB activation in part through zinc finger protein 440 (ZNF440) signaling and reductions in IκB expression. Modulation of the ZNF440/NF-κB axis (IκB-independent regulation of NF-κB) and IκB-dependent regulation of NF-κB by miR-181a-5p and miR-4454 signaling in FJ OA chondrocytes may be crucial in contributing to the progressive pathologies associated with OA, including cartilage degeneration.

OA chondrocytes (25, 26). Previous studies have also reported links between miR-181 and miR-4454 and NF-κB signaling in other cells and tissues. Activation of *STAT3*, an important component of the NF-κB signaling pathway, increases miR-181 expression in cancer cells (27), while NF-κB regulates the expression of miR-181 in breast tumor cells (28). A study performed in TNF-α–stimulated HeLa cells also identified miR-4454 as a NF-κB target miRNA (29). Our computational approach using pathway enrichment analysis also predicted close association of the NF-κB pathway with both miR-181a-5p and miR-4454. Indeed, our results showed that FJ OA chondrocytes treated with IL-1β enhanced phosphorylation of Ser536 of NF-κB p65, which promotes NF-κB p65 activity independent of IκB expression (21), and increased the expression of miR-181a-5p and miR-4454. We found that these miRNAs alone also increased phosphorylation of Ser536 NF-κB p65 through increased expression of *ZNF440* and reduced the expression of IκBα, an inhibitor of NF-κB p65 nuclear localization and activity (20). Overall, these observations suggest that IL-1β–mediated activation of NF-κB signaling may upregulate miR-181a-5p and miR-4454 expression to sustain NF-κB activation, in part, through *ZNF440*-mediated phosphorylation of Ser536 NF-κB p65 and reduction of IκB expression, resulting in a positive feedback loop that can sustain NF-κB p65 activity. Thus, expression of miR-181a-5p and miR-4454 appears critical for regulating both canonical NF-κB signaling (IκB dependent) and the ZNF440/NF-κB axis (IκB independent) in FJ OA chondrocytes. A model of sustained NF-κB signaling induced by IL-1β is provided in Figure 6.

Our in vitro data using miR-181a-5p and miR-4454 mimics or inhibitors strongly suggested that these miRNAs promote cartilage degenerative effects in FJ OA chondrocytes. To prove this in vivo, we performed an intra-articular injection of miR-181a-5p mimic into L4/5 and L5/6 spinal levels in rats. At 3 weeks after injection, FJ cartilage treated with miR-181a-5p mimic exhibited a FJ OA phenotype associated with substantial cartilage degeneration, excessive loss of chondrocytes, proteoglycan depletion, enhanced chondrocyte apoptosis (PARP p85 immunostaining), and increased cartilage catabolic activity (MMP13 immunostaining). These findings further consolidate the ability of miR-181a-5p to mediate facet cartilage degeneration in vivo by promoting cell death and cartilage destructive activity and also represent a viable in vivo experimental model for FJ degeneration. However, it remains to be determined if miR-181a-5p mimic causes facet cartilage degeneration by direct cartilage/chondrocyte uptake or via other surrounding tissues.

It is critical to highlight limitations of this study. First, during the screening stage of miRNA array analysis, only $n = 2$ control cartilage specimens were analyzed compared with FJ OA cartilage specimens comprising of two pooled samples from $n = 3$ separate cartilage specimens. Use of additional pooled cartilage specimens in the control group may have increased the scope of screening of miRNAs by array analysis. Second, validation analyses were performed on only 7 miRNAs exhibiting greater than 2-fold difference in the expression between control and FJ OA cartilage during screening phase. Though beyond the scope of this study, it would be worthwhile to test the expression of other miRNAs with less than a 2-fold change between control and FJ OA cartilage to identify potential differences in the expression of other miRNAs and their contribution to FJ OA. Third, due to the specialized nature of this surgery, a low number of patients were enrolled in this study, resulting in $n = 21$ control and $n = 34$ FJ OA patient samples. Future studies should be directed to test the expression and regulation of miR-181a-5p and miR-4454 in a larger patient cohort. Finally, this study was also unable to determine the exact relationship between age and the expression of miR-181a-5p and miR-4454, as the control group consisted of LDH patients with an age range of 24 to 53 years old compared FJ OA patients with an age range of 42 to 81 years old.

Since the FJ OA group exhibited a higher age range and greater expression of miR-181a-5p and miR-4454 compared with the low expression levels of miR-181a-5p and miR-4454 determined in the control group with a lower age range, a study of the direct correlation between age and the expression of these miRNAs could not be performed.

Overall, this study provides the first comprehensive evidence to our knowledge of miR-181a-5p and miR-4454 as potential mediators of cartilage degeneration as well as therapeutic targets to counteract cartilage degeneration during FJ OA. The fact that both miR-181a-5p and miR-4454 are substantially elevated in FJ OA cartilage and exhibit a positive correlation with disease severity, as assessed by MRI, indicates the potential of these two miRNAs as markers of cartilage degeneration, warranting further investigation. Though beyond the scope of this study, the next logical step would be to test the expression of circulating miR-181a-5p and miR-4454 in the sera/plasma of patients with varying degrees of FJ OA; this would allow a comprehensive exploitation of their potential as clinical markers to detect cartilage degeneration. This study also investigated the expression and regulation of miRNAs in FJs; however, expression and regulation of miR-181a-5p and miR-4454 should also be tested in other joints affected by OA, such as knee or hip, to determine if these miRNAs exhibit similar or distinct regulation in other OA joints compared with FJs. Finally, inhibitors of these two miRNAs should be tested in vivo using animal models of facet cartilage degeneration to determine the therapeutic potential of miR-181a-5p and miR-4454 inhibition in reducing or delaying facet cartilage degeneration.

Methods

Patient information. The medial aspect of FJs were obtained from spinal level L3-S1 of FJ OA patients (n = 34; age range: 42–81 years, mean age ± SEM: 65.5 ± 1.6 years) undergoing lumbar surgery for neurogenic claudication due to LSS caused by FJ OA. In addition, FJs were obtained from spinal level L4-S1 of LDH patients (n = 21; age range: 24–53 years old, mean age ± SEM: 34.1 ± 1.4 years old) undergoing microdiscectomy (control group). Patients with infection or inflammatory/autoimmune diseases were excluded. Relevant surgical spine level(s) were determined from standard clinical and imaging assessment, as per standard surgical practice. The degree of degeneration in the FJ and intervertebral disc on routine preoperative MRIs was independently assessed and graded by two spine surgeons (YRR and SJL) using the grading systems described by Weishaupt et al. (16) and Pfirrmann et al. (17), respectively (Table 1).

Histopathology. The degree of FJ cartilage degeneration was determined by histological analysis. FJ specimens from humans and rats were fixed in formalin for at least 72 hours, decalcified in 0.5 M Hydrochloric acid (BioShop) with 0.1% Glutaraldehyde (Sigma-Aldrich) for 7 days for human samples and Rapid Decalcifier (Apex Engineering) for 3 hours for rat samples, respectively, and embedded in paraffin. Serial sections (5 μm) were stained with Safranin O (Sigma-Aldrich)/Fast green (Bio Basic Canada Inc.) staining and evaluated by two blinded observers using the OARSI grading score (18).

Immunohistochemistry and TUNEL staining. Five-micron sections were deparaffinized in xylene followed by a graded series of alcohol washes. Endogenous peroxide was blocked for 5 minutes using 1% H_2O_2 for 30 minutes. Nonspecific IgG binding was blocked by incubating sections with BSA (0.1%) in PBS for 30 minutes. Sections were then incubated with primary antibodies for PARP p85 (PROMEGA, catalog G734) (dilution: 1:100), MMP13 (ABCAM, catalog ab39012) (dilution: 1:50) or rabbit IgG-HRP (Santa Cruz, catalog sc2749) (dilution: 1:50 or 1:100) as an isotype negative control in a humidified chamber and left overnight at 4°C. After washing twice in water, the slides were incubated with their respective biotinylated secondary antibodies for 30 minutes. Signal was amplified with HRP-conjugated secondary antibody, followed by incubation using the Vectastain Elite ABC kit (Vector Laboratories), as per manufacturer's direction, and counterstained with eosin Y (Fisher Scientific). TUNEL assay was performed using the ApopTag Plus Peroxidase In Situ Apoptosis Detection Kit (Millipore, catalog S7101) according to the manufacturer's directions. The quantification of the number of positive cells for each antigen was performed by counting of the total number of chondrocytes and the total number that stained positive for the antigen for at least 4 replicates. The final results were expressed as the percentage of positive cells for each antigen.

RNA extraction from human FJ cartilage. For RNA extraction, fresh human FJ cartilage was immediately separated from the subchondral bone using a sterile scalpel blade and forceps under a dissection microscope (SMZ-168 series, Motic). FJ cartilage was snap frozen in liquid nitrogen and homogenized using the Cellcrusher tissue pulverizer (Cellcrusher), with the barrel and ball precooled in liquid nitrogen. The total RNA from FJ cartilage or chondrocytes was isolated using TRIzol reagent (Invitrogen), followed by use of

the RNeasy Mini kit clean-up for purification (Qiagen), according to the manufacturers' protocols.

miRNA microarray. Microarray and data analysis were conducted at Exiqon Services, Denmark. The miRNA screening was performed using a seventh generation miRCURY LNA miRNA Array (Exiqon) containing capture probes targeting all human miRNAs annotated in miRBase 20.0. Four samples of total RNA extracted from human facet cartilage (n = 2 from FJ OA and n = 2 from control groups) were subjected to the miRNA arrays. In FJ OA group, each sample consisted of pooled cartilage samples from n = 3 separate FJ OA patients.

Briefly, total RNA from cartilage, isolated as described above, was used for hybridization. The quality of the total RNA was verified by an Agilent 2100 Bioanalyzer profile. A total of 400 ng RNA from each sample was labeled with Hy3 fluorescent label, using the miRCURY LNA miRNA Hi-Power Labeling Kit, Hy3/Hy5 (Exiqon). The Hy3-labeled samples and a Hy5-labeled reference RNA sample were mixed pairwise and hybridized to the array. Hybridization was performed using a Tecan HS 4800 hybridization station (Tecan). The miRCURY LNA array slides were scanned using the Agilent G2565BA Microarray Scanner System (Agilent Technologies Inc.), and image analysis was carried out using the ImaGene 9.0 software (miRCURY LNA microRNA Array Analysis Software, Exiqon). Quantified signals were background corrected (normexp with offset value 10) and normalized using the global locally weighted scatterplot smoothing (LOWESS) regression algorithm. Following normalization, principal component analysis, traditional and matrix plots, and heatmap hierarchical clustering were obtained.

Reverse transcription and RT-PCR. For RT-PCR, RNA concentrations were determined using Nano-Drop 1000 (Thermo Scientific) and NanoVue (GE Healthcare Life Science). Following RNA quantification, equal amounts of RNA (400 ng for mRNA and 10 ng for miRNA expression analysis) were converted to cDNA using the QuantiTect Reverse Transcription PCR Kit (Qiagen) for mRNAs or the Universal cDNA synthesis kit II (Exiqon) for miRNAs, as per the manufacturers' directions. For RT-PCR reactions, 5 ng RNA per well was used for mRNA with primers and SYBR Green Master Mix (BIO-RAD), and 0.2 ng RNA per well was used for miRNA with primers and SYBR Green Master Mix Kit (Exiqon) according to the manufactures' protocols. The reactions were incubated in 96-well plates (BIO-RAD), and all reactions were performed in duplicates. Specificity of the amplified RT-PCR product was assessed by performing melting curve analysis on the LightCycler 480 Instrument. The relative expression of PCR products was calculated by the $2^{-\Delta Ct}$ method. All primers were designed using Primer3 online software (Supplemental Table 6). Data were normalized to GAPDH for mRNA and to hsa-U6 snRNA for miRNA analyses, respectively. Both reference genes showed highly stable expression compared with other candidates for reference genes. For some highly degenerated FJ OA cartilage specimens, pooled cartilage from at least two patient samples were used to extract adequate amount of RNA for RT-PCR analysis.

FJ chondrocyte treatment with miRNA mimics, inhibitors, or siRNA. Chondrocytes were extracted from FJ cartilage obtained from FJ OA patients as previously described (30). Primary chondrocytes were cultured for 14 to 21 days in DMEM (Invitrogen) containing 10% FBS and 1% penicillin/streptomycin at 37°C in a humidified atmosphere of 5% CO_2 and 95% air. Medium was changed every 2 to 3 days. Confluent cultures were detached with 0.05% trypsin and plated at a density of 1×10^5 cells/well in 6-well plates.

For mimic studies, cells were treated with 5 nM miRCURY LNA Mimic for miR-181a-5p (hsa-miR-181a-5p), miR-4454 (hsa-miR-4454), or control (cel-miR-39-3; cel-miR-39-3p has no homology to any known miRNA or mRNA sequences in mouse, rat, or human; all from Exiqon) for 24 hours using TransFectin Lipid Reagent (BIO-RAD) (1 μg/ml) according to the manufacturer's instructions. For inhibition studies, cells were treated with recombinant human IL-1β (10 ng/ml; R&D Systems) for 18 hours, followed by transfection with 50 nM miRCURY LNA Power microRNA inhibitor (antisense oligonucleotides) for miR-181a-5p or miR-4454 or negative control A (Exiqon) for 24 hours. Total RNA and proteins were isolated using TRIzol reagent (Invitrogen) or RIPA buffer (Sigma-Aldrich), respectively.

Twenty-four hours after seeding, first-passage human facet chondrocytes were serum starved for 3 hours and cotransfected with miR-181a-5p or miR-4454 mimic (both at 5 nM) and ZNF440 siRNA (siZNF440) (50 nM) (Santa Cruz, catalog sc97725) or control siRNA (50 nM) (Qiagen, catalog 1027280; this siRNA has no homology to any known mammalian gene) using TransFectin Lipid Reagent (BIO-RAD) (10 μg/ml) in 0.5% of FBS and 1% penicillin/streptomycin media. After 48 hours of cotransfection, cells were washed 3 times with PBS and cell lysates were collected in RIPA buffer (Sigma-Aldrich).

miRNA target and pathway enrichment analysis. We used mirDIP (31) version 2.0 (http://ophid.utoronto.ca/mirDIP) to identify the most likely targets of miR-181a-5p and miR-4454, focusing only on middle

third, top third, and top 1% targets. The network was visualized using NAViGaTOR (32) version 2.3 (http://ophid.utoronto.ca/navigator). Selected targets were then subjected to pathway enrichment analysis using pathDIP version 1.0 (http://ophid.utoronto.ca/pathDIP).

Western blot analysis. Cell lysates in RIPA buffer were applied to SDS-polyacrylamide gels (10%–15%) for electrophoresis. Separated protein was electroblotted onto polyvinylidene fluoride membranes. Membranes were blocked in 10 mM Tris-buffered saline (TBS) containing 5% skimmed milk and probed for 1.5 hours with rabbit polyclonal IgG primary antibodies (1: 500) specific for NF-κB p65 (Santa Cruz, catalog sc109), phospho-NF-κB p65 (Ser536) (Cell Signaling, catalog 3031), IκBα (Santa Cruz, catalog sc371), or PARP p85 (PROMEGA, catalog G734), or mouse monoclonal IgG (1:1,000) for β-actin (Sigma-Aldrich, catalog A1978) in blocking buffer. After washing the membranes with TBS containing 0.1% Tween-20 (TBS-T) 3 times, the membranes were incubated overnight at 4°C with HRP-conjugated anti-rabbit (1:5,000; Sigma-Aldrich, catalog SAB3700843) or anti-mouse (1:10,000; Sigma-Aldrich, catalog A2179) secondary antibodies in TBS containing 5% skimmed milk. Membranes were subsequently washed in TBS-T, and protein bands were visualized with an enhanced chemiluminescence substrate (Clarify Western ECL Substrate, BIO-RAD, and SuperSignal West Pico, Thermo Science) using a BIO-RAD Chemidoc Apparatus. Blots were scanned, and signal intensity was quantified using ImageJ (National Institutes of Health, USA).

Injection of miR-181a-5p into lumbar FJs of rats. Male Sprague-Dawley rats (200–220 g; n = 7/group; Charles River Canada) were anesthetized with 2.0% isoflurane in oxygen in the prone position. Following a 2-cm midline skin incision, right paraspinal muscles were retracted, exposing the left L4/L5 and L5/L6 FJs (most common levels affected in lumbar FJ OA), and injected intra-articularly with miRCURY LNA mimic hsa-miR-181a-5p in vivo Ready (2 μl of 2.5 μg/μl; Exiqon) through the facet capsular tissue using a 26-gauge Hamilton syringe. Left FJs at identical levels were injected with miRCURY LNA mimic cel-miR-39-3p LNA in vivo Ready (control mimic) (2 μl of 2.5 μg/μl; Exiqon). Rats in the sham group only underwent a surgical incision without injection. Rats were sacrificed at 3 weeks after surgery/injection for histological and immunohistochemical analysis.

Accession numbers. The data supporting the results of this article are available in the NCBI's GEO repository (GEO accession: GSE79258) for facet cartilage miRNA array analysis (http://www.ncbi.nlm.nih.gov/geo/query/acc.cgi?acc=GSE79258).

Statistics. Data are presented as box-and-whiskers plots, with the horizontal lines and cross marks representing the medians and the means, respectively. The upper and lower bounds of the box correspond to the 25th and 75th percentiles of the data set. The whiskers denote the minimum and maximum values of the data set. The patient average age in the control group and the FJ OA group is presented as mean ± SEM. Difference in the expression of miRNAs and mRNAs (isolated from FJ cartilage or FJ OA chondrocytes treated with miR mimics) was analyzed by 2-tailed Student's t test. Differences in the expression levels of markers in response to miR-181a-5p and miR-4454 inhibition with or without IL-1β and cotransfection with miRNA mimics and siRNA treatments were determined by 1-way analysis of variance, followed by Tukey's honest significant difference post-hoc test. The significance of the correlation between the expression of miR-181a-5p or miR-4454 and severity of FJ OA based on MRI grading score was determined by 2-tailed t-test of the miRNA coefficient in each ordinal regression model. Correlations between miR-181a-5p or miR-4454 expression and FJ OA MRI grade were assessed with Spearman's rank-order correlation coefficient. The χ^2 test was used to evaluate differences in FJ OA and disc degeneration between the control and FJ OA groups. A value of $P < 0.05$ was considered statistically significant for all comparison tests.

Study approval. The human facet cartilage study was approved by the Institutional Research Ethics Board Committee, University Health Network. Informed consent to participate in this study was obtained from all patients. The animal experiments were approved by the Animal Resources Centre, University Health Network.

Author contributions

AN was involved in the conception and design of the study, acquisition of data, analysis and interpretation of data, drafting the article, revising it critically for important intellectual content, and approved the final version of the manuscript. YRR was involved in the design of the study, performed spine surgery in patients with LSS or LDH, provided tissues, performed MRI grading, drafted the article, revised it critically for important intellectual content, and approved the final version of the manuscript. SJL performed spine surgery in patients with LSS or LDH, provided tissues, performed MRI grading along with YRR, drafted

the article, revising it critically for important intellectual content, and approved the final version of the manuscript. AS performed animal surgeries to inject miRNA mimics, performed tissue dissections along with AN, drafted the article, revising it critically for important intellectual content, and approved the final version of the manuscript. KS performed the statistical analysis, drafted the article, revising it critically for important intellectual content, and approved the final version of the manuscript. BW performed cell culture studies with AN, drafted the article, revising it critically for important intellectual content, and approved the final version of the manuscript. ER, PD, and HE performed histology, immunohistochemistry, and TUNEL assays of human and rat samples, drafted the article, revising it critically for important intellectual content, and approved the final version of the manuscript. JSR was involved in the interpretation of data, drafting the article, revising it critically for important intellectual content, and approved the final version of the manuscript. IJ performed computational, gene prediction, and pathway enrichment analysis, drafted the article, revising it critically for important intellectual content, and approved the final version of the manuscript. MK was involved in the conception and design of the study, interpretation of data, drafting the article, revising it critically for important intellectual content, and approved the final version of the manuscript.

Acknowledgments

The authors would like to thank Amanda Weston, Kim Perry, Erdeta Prifti, Luis Montoya, Daniel Antflek, and Oma Persaud for their help with collecting facet cartilage and patient data collection. The authors would also like to acknowledge the help of members of the Arthritis Program at the Toronto Western Hospital. This study was supported by The Arthritis Program, University Health Network, and the Krembil Foundation. IJ is supported in part by the Canada Research Chair Program (CRC 203373 and 225404), the Canada Foundation for Innovation (CFI 12301, 203373, 29272, 225404, 30865), and IBM. AN is a recipient of a postdoctoral fellowship from the Krembil Research Institute.

Address correspondence to: Mohit Kapoor, Arthritis Program, University Health Network, Department of Surgery and Department of Laboratory Medicine and Pathobiology, University of Toronto; Division of Genetics and Development, Krembil Research Institute, 60 Leonard Avenue, Toronto, Ontario, M5T 2S8, Canada. Phone: 416.603.5800 ext. 4796; E-mail: Mohit.Kapoor@uhnresearch.ca.

1. Suri P, Hunter DJ, Rainville J, Guermazi A, Katz JN. Presence and extent of severe facet joint osteoarthritis are associated with back pain in older adults. *Osteoarthr Cartil*. *2013;21(9):1199–1206*.
2. Miyaki S, et al. MicroRNA-140 is expressed in differentiated human articular chondrocytes and modulates interleukin-1 responses. *Arthritis Rheum*. 2009;60(9):2723–2730.
3. Lee Y, Jeon K, Lee JT, Kim S, Kim VN. MicroRNA maturation: stepwise processing and subcellular localization. *EMBO J*. 2002;21(17):4663–4670.
4. Lee Y, et al. The nuclear RNase III Drosha initiates microRNA processing. *Nature*. 2003;425(6956):415–419.
5. Voinnet O. Origin, biogenesis, and activity of plant microRNAs. *Cell*. 2009;136(4):669–687.
6. Johnnidis JB, et al. Regulation of progenitor cell proliferation and granulocyte function by microRNA-223. *Nature*. 2008;451(7182):1125–1129.
7. Sun L, et al. MicroRNA-34a suppresses cell proliferation and induces apoptosis in U87 glioma stem cells. *Technol Cancer Res Treat*. 2012;11(5):483–490.
8. Anderson RM. A role for dicer in aging and stress survival. *Cell Metab*. 2012;16(3):285–286.
9. Nugent M. MicroRNAs: exploring new horizons in osteoarthritis. *Osteoarthr Cartil*. 2016;24(4):573–580.
10. Wienholds E, et al. MicroRNA expression in zebrafish embryonic development. *Science*. 2005;309(5732):310–311.
11. Tuddenham L, et al. The cartilage specific microRNA-140 targets histone deacetylase 4 in mouse cells. *FEBS Lett*. 2006;580(17):4214–4217.
12. Miyaki S, et al. MicroRNA-140 plays dual roles in both cartilage development and homeostasis. *Genes Dev*. 2010;24(11):1173–1185.
13. Yamasaki K, et al. Expression of MicroRNA-146a in osteoarthritis cartilage. *Arthritis Rheum*. 2009;60(4):1035–1041.
14. Li J, et al. miR-146a, an IL-1β responsive miRNA, induces vascular endothelial growth factor and chondrocyte apoptosis by targeting Smad4. *Arthritis Res Ther*. 2012;14(2):R75.
15. Beyer C, et al. Signature of circulating microRNAs in osteoarthritis. *Ann Rheum Dis*. 2015;74(3):e18.
16. Weishaupt D, Zanetti M, Boos N, Hodler J. MR imaging and CT in osteoarthritis of the lumbar facet joints. *Skeletal Radiol*. 1999;28(4):215–219.
17. Pfirrmann CW, Metzdorf A, Zanetti M, Hodler J, Boos N. Magnetic resonance classification of lumbar intervertebral disc degeneration. *Spine*. 2001;26(17):1873–1878.
18. Pritzker KP, et al. Osteoarthritis cartilage histopathology: grading and staging. *Osteoarthr Cartil*. 2006;14(1):13–29.
19. Kapoor M, Martel-Pelletier J, Lajeunesse D, Pelletier JP, Fahmi H. Role of proinflammatory cytokines in the pathophysiology of osteoarthritis. *Nat Rev Rheumatol*. 2011;7(1):33–42.
20. Beg AA, Ruben SM, Scheinman RI, Haskill S, Rosen CA, Baldwin AS. I kappa B interacts with the nuclear localization

sequences of the subunits of NF-kappa B: a mechanism for cytoplasmic retention. *Genes Dev*. 1992;6(10):1899–1913.
21. Sasaki CY, Barberi TJ, Ghosh P, Longo DL. Phosphorylation of RelA/p65 on serine 536 defines an I{kappa}B{alpha}-independent NF-{kappa}B pathway. *J Biol Chem*. *2005;*280(41):34538–34547.
22. Sumiyoshi K, et al. Novel role of miR-181a in cartilage metabolism. *J Cell Biochem*. 2013;114(9):2094–2100.
23. Gabler J, Ruetze M, Kynast KL, Grossner T, Diederichs S, Richter W. Stage-specific miRs in chondrocyte maturation: differentiation-dependent and hypertrophy-related miR clusters and the miR-181 family. *Tissue Eng Part A*. 2015;21(23-24):2840–2851.
24. Song J, Lee M, Kim D, Han J, Chun CH, Jin EJ. MicroRNA-181b regulates articular chondrocytes differentiation and cartilage integrity. *Biochem Biophys Res Commun*. 2013;431(2):210–214.
25. Baugé C, Attia J, Leclercq S, Pujol JP, Galéra P, Boumédiene K. Interleukin-1beta up-regulation of Smad7 via NF-kappaB activation in human chondrocytes. *Arthritis Rheum*. 2008;58(1):221–226.
26. Agarwal S, et al. Role of NF-kappaB transcription factors in antiinflammatory and proinflammatory actions of mechanical signals. *Arthritis Rheum*. 2004;50(11):3541–3548.
27. Iliopoulos D, Jaeger SA, Hirsch HA, Bulyk ML, Struhl K. STAT3 activation of miR-21 and miR-181b-1 via PTEN and CYLD are part of the epigenetic switch linking inflammation to cancer. *Mol Cell*. 2010;39(4):493–506.
28. Kastrati I, Canestrari E, Frasor J. PHLDA1 expression is controlled by an estrogen receptor-NFκB-miR-181 regulatory loop and is essential for formation of ER+ mammospheres. *Oncogene*. 2015;34(18):2309–2316.
29. Zhou F, Wang W, Xing Y, Wang T, Xu X, Wang J. NF-κB target microRNAs and their target genes in TNFα-stimulated HeLa cells. *Biochim Biophys Acta*. 2014;1839(4):344–354.
30. Zhang Y, et al. Cartilage-specific deletion of mTOR upregulates autophagy and protects mice from osteoarthritis. *Ann Rheum Dis*. 2015;74(7):1432–1440.
31. Shirdel EA, Xie W, Mak TW, Jurisica I. NAViGaTing the micronome--using multiple microRNA prediction databases to identify signalling pathway-associated microRNAs. *PLoS One*. 2011;6(2):e17429.
32. Brown KR, et al. NAViGaTOR: Network Analysis, Visualization and Graphing Toronto. *Bioinformatics*. 2009;25(24):3327–3329.